https://doi.org/10.17221/71/2019-RAE

A study of nanomaterial transportation in the soil by finite difference approximations

Jaldair Araújo e Nóbrega[1], André Luis dos Santos Hortelan[1], Carlos Henrique Portezani[2], Eriton Rodrigo Botero[1]*

[1]Applied Optics Group, Faculty of Science and Technology, Federal University of Grande Dourados (UFGD), Dourados, Mato Grosso do Sul, Brazil

[2]Mato Grosso do Sul State University (UEMS), Dourados, Mato Grosso do Sul, Brazil

**Corresponding author: jaldair@gmail.com*

Citation: Nóbrega J.A., Hortelan A.L.S., Portezani C.H., Botero E.R. (2020): A study of nanomaterial transportation in the soil by finite difference approximations. Res. Agr. Eng., 66: 146–155.

Abstract: Although there has been an increase in the production and use of nanomaterials; few studies have analysed their contact with the environment and the consequent effects on an ecosystem's health, ranging from the impact on the growth of organisms to the contamination of water reservoirs. This work proposes a tool to study the transportation of nanomaterials in the soil by the finite difference method, modelling the dispersion of nanomaterials into the soil layers to estimate the environmental impact. The model validation was conducted through numerical simulations of manganese and zinc in contact with a compacted latosol. The results show that the nanoparticle pollutants move slowly through the layers and the highest concentration is found close to the source. Also, the Mn nanoparticles are in higher concentration than Zinc nanoparticles as a function of depth in the soil layers. The method generates more accurate simulated results in less time and provides a low-cost prediction of the environmental impact. Furthermore, the estimated environmental impacts can be used as a first approximation for the mitigation of the degraded area.

Keywords: transport computer simulation; latosol; environmental impact estimative; numerical solution

Nanomaterials are chemical substances or materials that are manufactured and used at a very small scale, i.e., 1 to 100 nm in at least one dimension (Saleh 2020), and they have been used in important economic segments such as electronics, cosmetics, agronomics, and the medical industry (Paschoalino et al. 2010; Noman et al. 2019; Ramos et al. 2019). Also, nanomaterials are gaining significance in technological applications due to their tunable chemical, physical, and mechanical properties and enhanced performance when compared with their bulkier counterparts and they can be classified into different groups based on various criteria such as those shown in Noman et al. (2017).

Contact with nanomaterials may affect the growth of the organisms inhabiting the soil, water sources and plants (Nogueira 2009; Bai 2012; Sagee et al. 2012; Fang 2013) The use of a model that represents the transport of water and solutes in the soil is important to understand and reduce groundwater and surface pollution. Furthermore, the possibility of predicting the movement of particles or solutes in the soil saves time and financial resources, which would be spent on experimental detection techniques (Oliveira 2000; Wu et al. 2020). However, due to a large number of variables, it is difficult to evaluate and represent their transport in the soil for various situations. In the literature, there are several models with different characteristics that aim to simulate water and solutes transport in the soil.

HYDRUS was presented in Yu and Zheng (2010) as a one-dimensional model to simulate the solute

https://doi.org/10.17221/71/2019-RAE

transport and soil water flow, using finite elements and convection and dispersion equations for salt movement in the soil. LEACHM is a model developed by Holden et al. (1996) that uses convection and dispersion equations indicated for homogeneous soils only. Kumar et al. (1998) created the model RZWQM designed to simulate soil transport and water flow. Oliveira (1999) developed a model to simulate the transport of water and solutes in the soil by the finite difference method that presents less deviations than the experimental results. SIMASS was created by Costa (1998) and is a three-dimensional model capable of simulating the transport of water and solutes in a non-permanent soil and was successfully tested in saturated soil.

Moreover, there are no soil transport parameters specifically for nanomaterials in the literature. The nanomaterials' contact with the soil is based on a flowing liquid, since they are almost dispersed in a liquid solution, through the pores of the soil with a laminar flow regime, being only turbulent in the apparent fractures (Silva et al. 2016). Assuming that the nanomaterials' movement in the soil can occur through advection, diffusion, or mechanical dispersion processes (also a combination of them), this work considers the hypothesis that numerical solutions could be formulated to predict the transportation and impacts by assuming different transport phenomena. Also, another hypothesis, which this work is based on, is that the experimental research values of manganese (Mn) and zinc (Zn) metals can be used, such as the results proposed by Azevedo et al. (2005) for the construction of a model that can be computationally simulated to provide data to determine and estimate the concentration of particles at different depths at different time intervals. Therefore, the objective of this manuscript is to develop a computational model of the nanomaterials' transport in the soil by numerical solutions of differential equations providing subsidies for research on the dynamics of nanomaterial movement in the soil.

MATERIAL AND METHODS

Transport equation. The one-dimensional movement of nanomaterials in the soil was considered and the transportation phenomena of advection and hydrodynamic dispersion was established as a first approximation for the displacement of the nanomaterials. The flow refers to the amount of nanoparticles' mass being transported through a volume of a soil in each instant of time. Advection consists of the transportation of a material or energy through a moving fluid, moving into the same direction of the flow lines and the velocity is equal to the average velocity of the percolating fluid (Freeze and Cherry, 1979). The advective flow, $\varnothing_A$, ($M{\cdot}L^{-2}{\cdot}T^{-1}$) is set as:

$$\varnothing_A = q \times C \quad (1)$$

where: A – advective flow; q – the flow of the solution or liquid containing the nanomaterials ($L{\cdot}T^{-1}$); C – the solute concentration ($M{\cdot}L^{-3}$).

Molecular diffusion is the process in which molecular and ionic constituents move in the direction of the concentration gradient. The molecules and ions move from higher to lower concentration regions, equilibrating the distribution of the solute in the solvent under thermal agitation (Silva et al. 2016). The diffusion stream can be expressed similarly to Fick's first law as:

$$\varnothing_D = - D_D \frac{\partial C}{\partial x} \quad (2)$$

where: $\varnothing_D$ – the diffusive flux ($M{\cdot}L^{-2}{\cdot}T^{-1}$); D_D – the molecular diffusion coefficient of a particle in water ($L^2{\cdot}T^{-1}$); e $\frac{\partial C}{\partial x}$ – the solute concentration gradient ($M{\cdot}L^{-4}$) referring to the coordinated x.

In liquid phases, the diffusion coefficient (D_D) is generally lower than the diffusion coefficient in pure water (D_0) (Braga Filho 2012). The liquid phase occupies parts of the soil, and in a saturation condition, this volume is equal to the volume of porosity. According to Reichardt (1996), the pores of the soils are tortuous, such that the length of the path traversed by the solute in the soil is significantly greater than a straight line to be traversed by in a medium containing just water (Hillel 1980). For the net portion of the diffusion coefficient (D_D), only multiplying the diffusion coefficient (D_D) by the volumetric moisture (θ; dimensionless) will get the ratio between the water and the total soil sample volume (Alvares, Alvarez 2009). Thus, the diffusion stream is described as:

$$\varnothing_D = - D_D \theta \frac{\partial C}{\partial x} \quad (3)$$

For explanation see Equation (2).

https://doi.org/10.17221/71/2019-RAE

For an unsaturated soil, when the volumetric moisture (θ) decreases, the volume fraction containing the liquid phase also decreases, consequently, the tortuosity of a soil is bigger. The diffusion coefficient can be estimated by:

$$D_D = D_0 \tau \tag{4}$$

where: D_D – the molecular diffusion coefficient in the soil solution ($L^2 \cdot T^{-1}$); τ – the tortuosity factor, proposed by Millington and Quirk (1961) as:

$$\tau = \frac{\theta^{\frac{10}{3}}}{\theta_s^2} \tag{5}$$

where: θ – the soil water content or volumetric moisture is equal to the liquid volume (L^{-3}) per the total soil volume (L^{-3}); θ_s^2 – the water content in the saturated soil or volume of the saturated soil which is equal to the liquid volume (L^{-3}) per the total volume of saturated soil (L^{-3}).

Mechanical dispersion is known as a phenomenon that causes the scattering of solutes due to variations in the velocity of the materials in a porous medium. It occurs when the fluid does not present a constant velocity equal to the advection speed. Through the similarity between the processes of molecular diffusion and mechanical dispersion, the equation describing the dispersive movement of solutes in the soil can be written as:

$$\varnothing_M = -D_M \theta \frac{\partial C}{\partial x} \tag{6}$$

where: θ_M – the dispersive flow ($M \cdot L^{-2} \cdot T^{-1}$); D_M – the mechanical dispersion coefficient ($L^{-2} \cdot T^{-1}$); for explanation see Equation (2).

Unlike molecular diffusion, which occurs in both static and dynamic conditions, mechanical dispersion occurs only in dynamic conditions, when there is movement of the solution (Prevedello 1996). The mechanical dispersion coefficient can be written in terms of the velocity of the solutions in the medium as:

$$D_M = \alpha v^n \tag{7}$$

where: α – dispersivity (L), v – average flow velocity of solutions in the soil ($L \cdot T^{-1}$); n – depends on the soil geometry.

The dispersity values are ruled by the experimental conditions. In a controlled soil column, this value between 0.5 and 2.0 cm and, for field conditions, this value may vary between 5 and 20 cm (Zeng, Bennet 2002). The average displacement velocity (v) can be defined in terms of the flow of the solution and the volumetric moisture, defined by θ:

$$v = \frac{q}{\theta} \tag{8}$$

For explanation see Equations (1 and 7).

Because they present similar effects in the transportation of materials, the molecular diffusion coefficients, and the dispersion coefficients can be added. The result is called the hydrodynamic dispersion coefficient (Kumar et al. 1998):

$$D = D_D + D_M \tag{9}$$

where: D – hydrodynamic dispersion coefficient; for explanation see Equations (2 and 6).

Adding the term of advection motion, the total flow can be represented by the sum of these terms, and are called the dispersive flux:

$$\varnothing_{Total} = \varnothing_A + \varnothing_D + \varnothing_M \tag{10}$$

For explanation see Equations (1 and 6).

Combining Equations (1, 3 and 6), we obtain the differential Equation that represents the solute general movement in the porous medium:

$$\varnothing_{Total} = -D\theta \frac{\partial C}{\partial x} + qC \tag{11}$$

For explanation see Equations (1, 3 and 6).

For the transient transportation of nanoparticles, the differential equations that describe the transportation should be obtained by conservation of the mass in terms of the continuity equation. Considering the solute that moves in direction x, per unit area and time, as shown in Figure 1, the amount of mass entering into the left face (M_E) is given by:

$$M_E = \varnothing_{Total} \Delta y \Delta z \tag{12}$$

where: Δy– width in the mass flow in a soil element; Δz – height in the mass flow in a soil element.

https://doi.org/10.17221/71/2019-RAE

The amount of the mass coming out (M_s) of the volume element, after crossing the entire volume, on the opposite face is:

$$M_S = \left[\varnothing_{\text{Total}} + \left(\frac{\partial \varnothing_{\text{Total}}}{\partial x} \Delta x \right) \right] \Delta y \Delta z \tag{13}$$

For explanation see Equations (11 and 12).

However, the difference between the amount of the solute as a function of time in the x-direction can be expressed by:

$$M_E - M_S = \varnothing_{\text{Total}} \Delta y \Delta z - \left[\varnothing_{\text{Total}} + \left(\frac{\partial \varnothing_{\text{Total}}}{\partial x} \Delta x \right) \right] \Delta y \Delta z =$$

$$= - \frac{\partial \varnothing_{\text{Total}}}{\partial \text{x}} \Delta x \Delta y \Delta z \tag{14}$$

where: M_s – mass coming out; for explanation see Equations (11 and 12).

Replacing Equation (11) in Equation (14), we will obtain:

$$M_E - M_S = \frac{\partial}{\partial x} \left(D\theta \frac{\partial \text{C}}{\partial x} - qC \right) \Delta x \Delta y \Delta z \tag{15}$$

For explanation see Equations (11 and 12).

Thus, the amount of nanomaterial accumulated into the volume is equal to $(\theta C + \rho S)\Delta x \Delta y \Delta z$, where the linear sorption (S) represents the amount of the solute that is retained in the soil.

The rate of the solute variation can be given by:

$$\frac{\partial}{\partial t} \left[\left(\theta C + \rho S \right) \Delta x \Delta y \Delta z \right] = \frac{\partial}{\partial x} \left(\text{D}\theta \frac{\partial C}{\partial x} - qC \right) \Delta x \Delta y \Delta z \tag{16}$$

For explanation see Equations (11 and 12).

By the principle of mass conservation according to Equation (16):

$$\frac{\partial}{\partial t} \left(\theta C + \rho S \right) = \frac{\partial}{\partial x} \left(\text{D}\theta \frac{\partial C}{\partial x} - qC \right) \tag{17}$$

For explanation see Equation (2).

Considering the linear sorption as $S = kC$, where k is the partition coefficient ($L^{-3} \cdot M^{-1}$) (Van, Wierenga 1986; Arias 2005; Lair 2006), and the permanent flow (constant q) in a homogeneous unsaturated soil profile, Equation (16) reduces to:

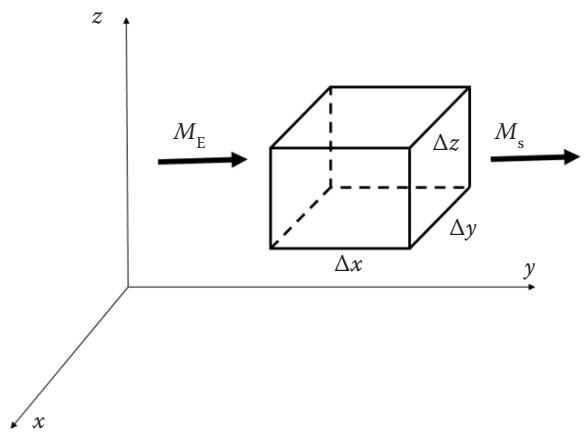

Figure 1. Representation of the mass flow in a soil element M_E– mass entering into the left face; M_s– mass coming out; x, y, z – directions

$$R \frac{\partial C}{\partial t} = D \frac{\partial^2 C}{\partial x^2} - v \frac{\partial C}{\partial x} \tag{18}$$

where: R – the lag factor defined by:

$$R = 1 + \frac{\rho k}{\theta} \tag{19}$$

where: k – the partition coefficient.

(20)

For the three-dimensional case, Equation (18) can be expanded as:

$$R \frac{\partial C}{\partial t} = D \left(\frac{\partial^2 C}{\partial x^2} + \frac{\partial^2 C}{\partial y^2} + \frac{\partial^2 C}{\partial z^2} \right) - v \left(\frac{\partial C}{\partial x} + \frac{\partial C}{\partial y} + \frac{\partial C}{\partial z} \right)$$

For explanation see Equations (2 and 18).

Discretisation by finite differences. The numerical deduction of the transport equation using the finite difference method is established through Equation (20). Applying the approximation by finite differences to the appropriate terms, and considering the first temporal derivative, the progressive difference applies (Fortuna 2012):

$$\frac{\partial c(x,y,z,t)}{\partial t} = \frac{c_{\text{i,j,k}}^{P+1} - c_{\text{i,j,k}}^{p}}{\Delta t} \tag{21}$$

where: c – the concentration value; t – time; for explanation see Equation (2).

The other spatial derivatives can obtain the central differences, such as:

https://doi.org/10.17221/71/2019-RAE

$$\frac{\partial c(x,y,z,t)}{\partial x} = \frac{c^{P}_{i+1,\,j,\,k} - c^{p}_{i-1,\,j,\,k}}{2\Delta x} \tag{22}$$

$$\frac{\partial c(x,y,z,t)}{\partial y} = \frac{c^{P}_{i,\,j+1,\,k} - c^{p}_{i,\,j-1,\,k}}{2\Delta y} \tag{23}$$

$$\frac{\partial c(x,y,z,t)}{\partial z} = \frac{c^{P}_{i,\,j,\,k+1} - c^{p}_{i,\,j,\,k-1}}{2\Delta z} \tag{24}$$

$$\frac{\partial^2 c(x,y,z,t)}{\partial x^2} = \frac{c^{P}_{i+1,\,j,\,k} - 2c^{p}_{i,\,j,\,k} + c^{p}_{i-1,\,j,\,k}}{(\Delta x)^2} \tag{25}$$

$$\frac{\partial^2 c(x,y,z,t)}{\partial y^2} = \frac{c^{P}_{i,\,j-1,\,k} - 2c^{p}_{i,\,j,\,k} + c^{p}_{i,\,j+1,\,k}}{(\Delta y)^2} \tag{26}$$

$$\frac{\partial^2 c(x,y,z,t)}{\partial z^2} = \frac{c^{P}_{i,\,j,\,k-1} - 2c^{p}_{i,\,j,\,k} + c^{p}_{i,\,j,\,k+1}}{(\Delta z)^2} \tag{27}$$

For explanation see Equations (2 and 21).

Considering $t = p\Delta t$ as the time given by the number of temporal increments p multiplied by the temporal variation Δt, replacing all the discretised terms in Equation (20):

$$c^{p+1}_{(i,j,k)} = \frac{D\Delta t}{R}\left[\begin{array}{l}\left(\dfrac{c^{p}_{(i+1,j,k)} - 2c^{p}_{(i,j,k)} + c^{p}_{(i-1,j,k)}}{(\Delta x)^2}\right) + \\ \left(\dfrac{c^{p}_{(i,j+1,k)} - 2c^{p}_{(i,j,k)} + c^{p}_{(i,j-1,k)}}{(\Delta y)^2}\right) + \\ \left(\dfrac{c^{p}_{(i,j,k+1)} - 2c^{p}_{(i,j,k)} + c^{p}_{(i,j,k-1)}}{(\Delta z)^2}\right)\end{array}\right] - \frac{v\Delta t}{R}\left[\begin{array}{l}\left(\dfrac{c^{p}_{(i+1,j,k)} - c^{p}_{(i-1,j,k)}}{2\Delta x}\right) \\ + \left(\dfrac{c^{p}_{(i,j+1,k)} - c^{p}_{(i,j-1,k)}}{2\Delta y}\right) + \\ \left(\dfrac{c^{p}_{(i,j,k+1)} - c^{p}_{(i,j,k-1)}}{2\Delta z}\right)\end{array}\right] + c^{p}_{(i,j,k)} \tag{28}$$

where: R – the lag factor; v – the average displacement velocity; for explanation see Equations (2 and 21).

Equation (28) can express a numerical solution for the transport equation of nanomaterials in the soil.

Validation of the results. The consistency test presented by Fortuna was used to verify that Equation (28) as a numerical solution for the differential one in Equation (20). To perform the consistency test, the concentrations of the numerical solutions were replaced by following expanded terms.

$$c^{p}_{(i\pm1,j,k)} = c^{p}_{(i,j,k)} \pm (\Delta x)\frac{\partial c}{\partial x} + \frac{(\Delta x)^2}{2!}\frac{\partial^2 c}{\partial x^2} \pm \pm \frac{(\Delta x)^3}{3!}\frac{\partial^3 c}{\partial x^3} + O(\Delta x)^4 \tag{29}$$

$$c^{p}_{(i\pm1,j,k)} = c^{p}_{(i,j,k)} \pm (\Delta y)\frac{\partial c}{\partial y} + \frac{(\Delta y)^2}{2!}\frac{\partial^2 c}{\partial y^2} \pm \pm \frac{(\Delta y)^3}{3!}\frac{\partial^3 c}{\partial y^3} + O(\Delta y)^4 \tag{30}$$

$$c^{p}_{(i\pm1,j,k)} = c^{p}_{(i,j,k)} \pm (\Delta z)\frac{\partial c}{\partial z} + \frac{(\Delta z)^2}{2!}\frac{\partial^2 c}{\partial z^2} \pm \pm \frac{(\Delta z)^3}{3!}\frac{\partial^3 c}{\partial z^3} + O(\Delta z)^4 \tag{31}$$

$$c^{p}_{(i\pm1,j,k)} = c^{p}_{(i,j,k)} \pm (\Delta t)\frac{\partial c}{\partial t} + \frac{(\Delta t)^2}{2!}\frac{\partial^2 c}{\partial t^2} + O(\Delta t)^3 \tag{32}$$

where: O – the limiting behavior of a function when the argument tends towards a particular value or infinity; for explanation see Equations (2 and 21).

Replacing each equation term in the discretised solution, the differential equation is given by:

$$R\frac{\partial c}{\partial t} = D\left(\frac{\partial^2 c}{\partial x^2} + \frac{\partial^2 c}{\partial y^2} + \frac{\partial^2 c}{\partial z^2}\right) - v\left(\frac{\partial c}{\partial x} + \frac{\partial c}{\partial y} + \frac{\partial c}{\partial z}\right) \tag{33}$$

For explanation see Equations (2 and 18).

The error:

$$-\frac{\Delta t^2}{2} \times \frac{\partial^2 c}{\partial t^2} - O(\Delta t)^2 + D\left[2O\left(\Delta x^2 + \Delta y^2 + \Delta z^2\right)\right] - v\left(\frac{\Delta x^2}{3}\cdot\frac{\partial^3 c}{\partial x^3} + \frac{\Delta y^2}{3}\cdot\frac{\partial^3 c}{\partial y^3} + \frac{\Delta z^2}{3}\cdot\frac{\partial^3 c}{\partial z^3}\right) \tag{34}$$

For explanation see Equations (2, 21 and 32).

Conditions for computational simulation. As observed in Equation (28), the concentration c of each cell receiving indices i, j, k (related, respectively, to the coordinates x, y, z, according to the formulations of the finite differences used) and, in the present index time $(p + 1)$, depends on the values of the concentration of the cell itself and the cells neighbouring it in an instant of the previous or part-time of the p index. This condition is exemplified in Figure 2. The concentration of cell A with coordinates (i, j, k)

https://doi.org/10.17221/71/2019-RAE

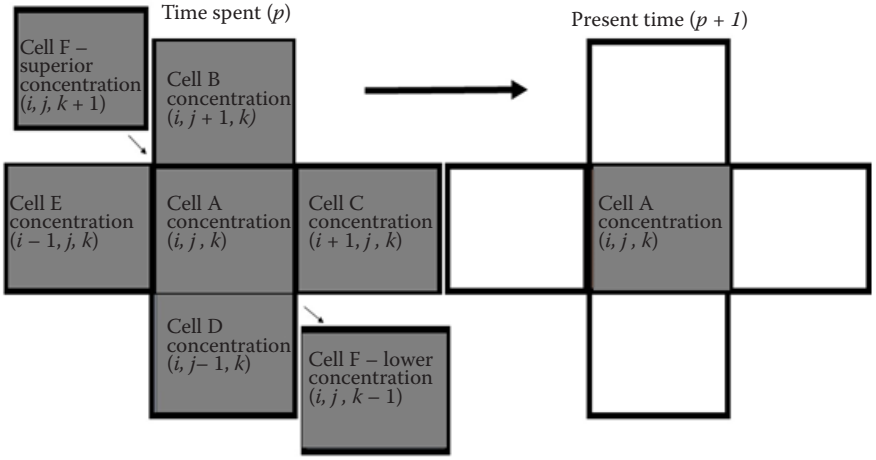

Figure 2. Schematic representation of the mass transfer process of a cell with indexes (*i, j, k*)

in the instant of the present time (p + 1) depends on the concentration of the neighbouring B, C, D, and E cells, and those located above cell F and below cell G and itself in the instant of the time spent (p) In this type of model, the transport of nanomaterials from a given source was formed through temporal increments (p). Thus, each cell had values for the concentrations changing at each moment of time Δt.

The nanoparticle disperses throughout a volume defined in the directions x, y, z or, respectively, in an initial way i, j, k, and can be attributed some conditions for the values of the concentrations of the cells located at the borders (i.e., at the extremities, on the vertices, edges, and faces of the analysed total volume) can be roughly calculated. Thus, instead of using the non-existent concentration value of the neighbouring cell in the time spent in Equation (28) in the border cells, the concentration value is used as being null at the moment passed ($c^{-p}_{(i, j, k)}$). With this, the modelling area becomes a limited dimension. Figure 3 shows the process of constructing the boundary conditions of the analysed volume. The arrows indicate the position where there are no cells, so the concentration in these locations receives values equal to zero. So, at the initial moment of analysis, the null values were assigned to the concentration values of the cells, except for the cells where the source was located, which, in this case, the concentration values were taken as being equal to the emission rate of the nanomaterial multiplied by the amount of time Δt, and the result is divided by the cell volume. Later in the analysis, when the values were equal to p multiplied by Δt, with $p > 1$, only one generation condition was assigned to the cells where the source is located as well as to all the cells of the analysed volume, thus, Equation (28) was respected with the appropriate restrictions for the border cells, as previously presented.

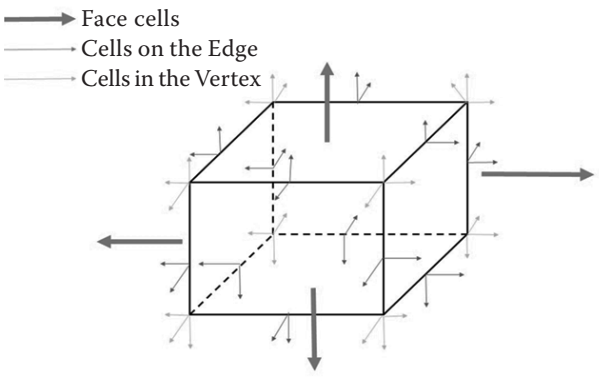

Figure 3. Scheme representing the construction of the border conditions

Parameters used for computational simulation. The model represents the transport of nanomaterials in soil that has been made in the Scilab programming environment (version 5.5.2). The transport parameters can be determined through laboratory experiments, such as column tests, diffusion tests, accumulated mass method, and an analysis based on numerical and analytical solutions. The value of the water velocity in the pores depends on the characteristics of the soil to be analysed, such as the porosity, tortuosity, and compaction. The transport parameters for the nanomaterials, in this research, were the extracted values of the experimental research of the metals Mn and Zn, through results proposed by Azevedo et al. (2005). Table 1 shows the parameters used for the computational simulation in this work.

https://doi.org/10.17221/71/2019-RAE

Table 1. Parameters used in the computational simulation for the compacted latosol soil

Reference	Parameter	Value
Transport	coefficient of hydrodynamic dispersion (D) – manganese	8.64×10^{-3} m^{-2}·s^{-1}
	coefficient of hydrodynamic dispersion (D) – zinc	6.42×10^{-3} m^{-2}·s^{-1}
	delay factor (R) – manganese	18.76 dimensionless
	delay factor (R) – zinc	27.05 dimensionless
	water velocity in the pores	1.667×10^{-4} m·s^{-1}
Source	dimension of the source on the x-axis	0.125 m
	dimension of the source on the y-axis	0.125 m
	dimension of the source on the y-axis	0.125 m
	number of source cells on the x-axis	1 u.a
	number of source cells on the y-axis	1 u.a
	number of source cells on the z-axis	1 u.a
	emission rate	1 g·s^{-1}·m^3
Dimensions of the modelled area	Δx	0.125 m
	Δy	0.125 m
	Δz	0.125 m
	distance on the x-axis before the source	10 m
	distance on the x-axis after the source	10 m
	distance on the y-axis before the source	10 m
	distance on the y-axis after the source	10 m
	distance on the z-axis before the source	0 m
	distance on the z-axis after the source	10 m
Time	Δt	1 s
	time to analyse	3 600 s

u.a – arbitrary unit

RESULTS AND DISCUSSION

Figure 4A shows the Mn simulation in water transportation at a depth of 0.0625 m, after a 1-hour simulation. The graphical representation gives the area occupied by the contaminant and the values of its concentration, in this case, 18 g·m^{-3}. Figure 4B shows the Mn being transported by water at a depth of 1.065 m after a 1-hour simulation, for the concentration values of 0.4 g·m^{-3}. Figure 5 shows the values for the Mn concentration up to 9. 0625 m in depth on the x coordinates and 0.125 m on the y coordinates, according to the simulation performed. The concentration of Zn for a 1-hour simulation is represented

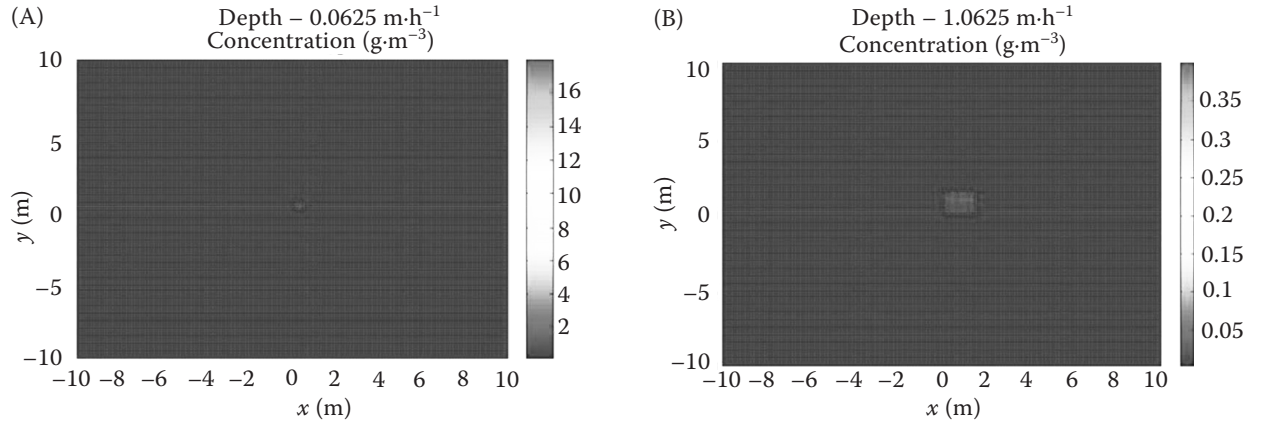

Figure 4. (A) Representation of the concentration of Mn in the soil at a depth of 0.0625 m and (B) representation of the concentration of Mn in the soil at a depth of 1.0625 m

https://doi.org/10.17221/71/2019-RAE

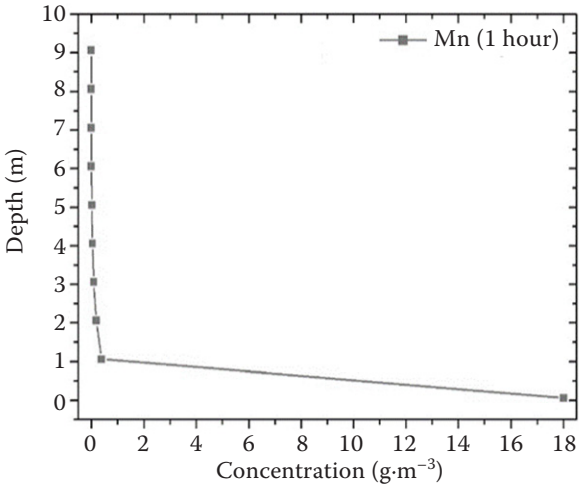

Figure 5. Concentration versus depth for the manganese with a simulation time of 1 hour

in Figure 6A. The concentration of Zn, in this case, reaches 14.5 g·m^{-3}. It can be observed in Figure 6B that the highest contamination (18 g·m^{-3}) occurs at a depth of 1.0625 m, and the lowest contamination (between 0 and 0.4 g·m^{-3}) occurs at a depth of 9.0625 m, demonstrating that the nanomaterials can move to the lower layers of the soil.

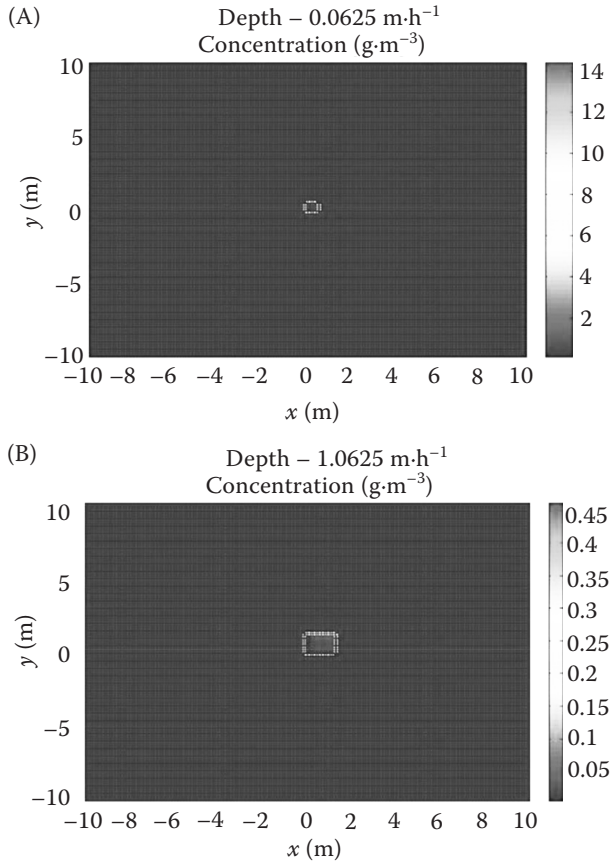

Figure 6. (A) Representation of the concentration of Zn in the soil at a depth of 0.0625 m and (B) representation of the concentration of Zn in the soil at a depth of 1.0625 m

The concentration of Zn after 1 hour at a depth of 1.0625 m is represented in Figure 6B and its values are 0.45 g·m^{-3}. Figure 7 presents the values for the concentration up to 10 m in depth with x and y coordinates being 0.125 m, according to the simulation performed. After the 1-hour simulation, it can be observed that the concentration of the manganese is higher than that of the zinc, this is mainly due to its higher retardation factor associated with its atomic structure by chemical processes and through the electrostatic interaction of zinc with the soil (Lima et al. 2007). However, this factor expresses the interactions between the liquid and solid phases that occur during the movement of the displacing solutions in the soil. The higher this factor, the greater the difficulty of the pollutant to move through the soil becomes (Boscov, Abreu 2000).

In the simulations for both 1 and 10 hours, it can be observed that the concentration presented by manganese is higher than that presented by zinc since it has a higher retardation factor related to its atomic structure, chemical processes, and its electrostatic interaction with the soil. However, this factor expresses the interactions between the liquid and solid phases that occur during the movement of the displacer solution in the soil. The higher this factor is, the greater the difficulty of the pollutant moving through the soil channels is.

The simulation shows an approximation of the real physical phenomenon since the soil type has a fundamental role in the transport of nanomaterials.

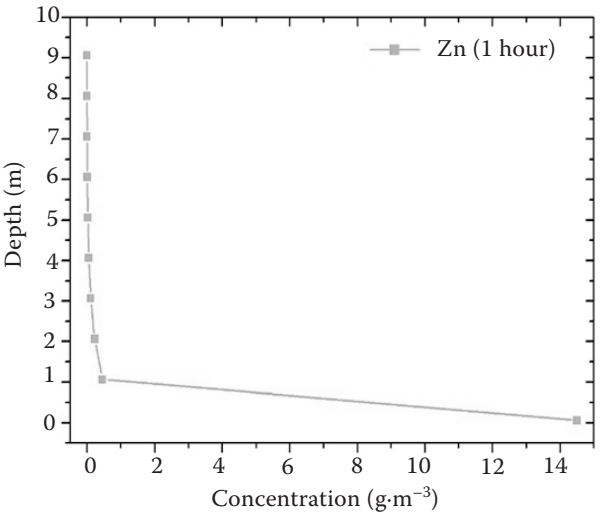

Figure 7. Concentration versus depth for the zinc with a simulation time of 1 hour

https://doi.org/10.17221/71/2019-RAE

According to Van Genuchten and Wierenga (1986), when the soil is little reactive, the pollutant is transported with the same speed with which the water transports the pollutant and, by the presented results, the speed value is low. On the other hand, according to Fetter (1994), the metals mostly have reasonably limited mobility in the soil, because there is an electrostatic interaction with the soil and the mineral grains. Therefore, the metal is concentrated near the emitting source.

The cation concentration in the solution of the soil favours competition between the retention sites favouring the transport of those that were not removed, which presents an imminent danger to the sources. The lower the velocity and flow density of the solutions, the greater the contact between the soil and the pollutant, the greater the retention or, also, the adsorption process. The source entered into the search is a point source, which has a specific location. This represents leaks through pipelines with the polluting materials, e.g., leakage from landfills and domestic sinks. The pollutant released by the point sources has a higher concentration than the other sources and a great capacity to reach the deeper layers of the soil, contaminating aquifers and water reservoirs depending on the pollutant being introduced to the soil (Matos 2010). The higher concentration of manganese than zinc occurs due to the transport through advection, which is to say that zinc has a greater capacity to move because the pollutant follows the same lines of flow the water that is carrying it in the type of transport. For manganese, the predominant process is that of diffusion, this process may be an indication that the manganese is retained as the water flow advances over the soil profile (Pinheiro et al. 2009).

CONCLUSION

The computational implementation can simulate the transport of nanomaterials in several types of soils. Its numerical solution can be obtained through the method by finite differences and can be computationally implemented. In the case of Mn and Zn nanoparticles that do not react or deposit in the soil, there were also influences of retardation factors and hydrodynamic dispersion coefficients on the concentration values. However, some considerations should be made, especially with the type of material interaction with the medium and to the type of soil studied. The technique presented may serve as a reference for the possible use of the soil and provide necessary information regarding the transport of nanomaterials by the soil layers. Thus, it is possible to estimate whether the soil loses its characteristics and how much material will be deposed in the soil profiles. Because it is a quick and inexpensive alternative, the implementation, in some cases, can substitute for the high-cost experimental techniques providing results in a shorter time interval, and moreover providing a preventive study where it is not necessary to have the nanomaterial come in contact with the soil.

Acknowledgement: To the Capes for the financial support for conducting the research.

REFERENCES

Alvares V.H., Alvarez G.A.M. (2009): Grandezas, Dimensões, Unidades (SI) e Constantes Utilizadas em Química e Fertilidade do Solo. Viçosa, Editora Produção Independente: 86.

Ramos R.R., Rodríguez B.S., Mayor A.S., Delgado M.A.R., (2019): Nanomaterials as alternative dispersants for the multiresidue analysis of phthalates in soil samples using matrix solid phase dispersion prior to ultra-high performance liquid chromatography tandem mass spectrometry: Chemosphere, 236: 124377.

Arias M., Pérez-Novo C., Osorio F., López E., Soto B. (2005): Absorption and desorption of cooper and zinc in the surface layer of acid soils. Journal of Colloid and Interface Science. 288: 21–29.

Azevedo I.C.D., Nascentes R.C., Matos T.A., Azevedo F.R. (2005): Determinação de parâmetros de transporte de metais pesados em Latossolo compactado. Revista Brasileira de Engenharia Agrícola e Ambiental, 9: 623–630.

Bai C., Li Y. (2012): Modeling the transport and retention of nC60 nanoparticles in the subsurface under different release scenarios. Journal of Contaminant Hydrology, 136–137: 43–55.

Boscov M.E.G., Abreu R.C. (2000): Aterros Sanitários – Previsão de Desempenho x Comportamento Real. São Paulo, ABMS/NRSP: 139.

Braga Filho W. (2012): Fenômenos de Transporte para Engenharia. São Paulo, Editora LTC: 856.

Costa S.N. (1998): Desenvolvimento de um modelo numérico para simulação do transporte de água e solutos no solo sob condições de escoamento não permanente na vertical [Ph.D. thesis]. Viçosa, Universidade Federal de Viçosa: 153.

Fang J., Xu M.J., Wang D., Wen B., Han J. (2013): Modeling the transport of TiO_2 nanoparticle aggregates in saturated

https://doi.org/10.17221/71/2019-RAE

and unsaturated granular media: Effects of ionic strength and pH. Water Research, 47: 1399–1408.

Fetter C.W. (1994): Applied Hydrogeology. New York, Macmillan College Publishing Company: 691.

Fortuna A.O. (2012): Técnicas Computacionais para Dinâmica dos Fluidos: Conceitos básicos e aplicações. São Paulo, Editora Edusp: 552

Freze R.A., Cherry J.A. (1979): Groundwater. Englewood Cliffs, Prentice-Hall: 604.

Hillel D. (1980): Fundamentals of Soil Physics. New York, Academic Press: 413

Holden N.M., Rook J.A., Scholefield D. (1996): Testing the performance of a one-dimensional solute transport model using response surface methodology. Geoderma, 69: 157–163.

Kumar A., Kanwar R.S., Ahuja L.R. (1998): RZWQM simulation of nitrate concentrations in subsurface drainage from manured plots. Transactions of the ASAE, 41: 587–597.

Lair G.J., Gerzabek M.H., Haberhauer G., Jakusch M., Kirchmann H. (2006): Response of the sorption behavior of Cu, Cd and Zn to different soil management. Journal of Soil Science and Plant Nutrition Science, 169: 60–68.

Matos A.T. (2010): Poluição Ambiental – Impactos no Meio Físico. Viçosa, Editora UFV: 260.

Lima C.G.R., Carvalho M.P., Mello L.M.M., Lima R.C. (2007): Correlação linear e espacial entre a produtividade de forragem, a porosidade total e a densidade do solo de Pereira Barreto (SP). Revista Brasileira de Ciência do Solo, 31: 1233–1244.

Millington R.J., Quirk J.M. (1961): Permeability of porous solids. Transactions of the Faraday Society, 57: 1200–1207.

Nogueira V.I.J.O. (2009): Impacto de nanomateriais orgânicos na estrutura da comunidade microbiana do solo [Ph.D. thesis]. Aveiro, Universidade de Aveiro: 45.

Noman M.T, Militky J., Wiener J., Saskova J., Ashraf M.A., Jamshaid H., Azeem M. (2017): Sonochemical synthesis of highly crystalline photocatalyst for industrial applications. Ultrasonics, 83: 203–213.

Noman M.T, Ashraf M.A., Ali A. (2019): Synthesis and applications of nano TiO_2: A review. Environmental Science and Pollution Research, 26: 3262–3291.

Oliveira L.F.C. (1999): Modelo para transporte de solutos no solo e no escoamento superficial. Viçosa, Universidade Federal de Viçosa: 171.

Oliveira L.F.C., Martinez M.A., Pruski F.F., Ruiz H.A., Lima L.A. (2000): Transporte de solutos no solo e no escoamento superficial – Desenvolvimento do modelo e simulação do movimento de água e escoamento superficial. Revista Brasileira de Engenharia Agrícola e Ambiental, 4: 63–69.

Paschoalino M.P., Marcone G.P.S., Jardim W.F. (2010): Os nanomateriais e a questão ambiental. Química Nova, 33: 421–430.

Pinheiro A., Gonçalves Jr. A.C., Wisniewski Jr. A., Moraes J.C.S., Silva M.R. (2009): Estudo da presença de pesticidas no perfil do solo, sob diferentes tipos de culturas. Revista Brasileira de Recursos Hídricos, 14: 51–59.

Prevedello C.L. (1996): Física de Solos com Problemas Resolvidos. Curitiba, Salesward-Discovery: 446.

Reichardt K. (1996): Dinâmica da matéria e da energia em ecossistemas. Piracicaba, EdUSP: 513.

Sagee O., Dror I., Berkowitz B. (2012): Transport of silver nanoparticles (AgNPs) in soil. Chemosphere, 88: 670–675.

Saleh T.A (2020): Nanomaterials: Classification, properties, and environmental toxicities. Environmental Technology & Innovation, 20: 101067.

Silva B.C.P., Vidal D.M., Queiroz P.I.B. (2004): Efeito da sorção no transporte de contaminantes orgânicos. Available at: http://www.bibl.ita.br/xencita/Artigos/24.pdf (Jan 28, 2014).

Van Genuchten M.T., Wierenga P.J. (1986): Solute dispersion: coefficients and retardation factors. In: Klute A. (ed.): Methods of Soil Analysis: Part 1: Physical and Mineralogical Methods. Madison, ASA-SSSA Publisher: 1025–1031.

Yu C., Zheng C. (2010): HYDRUS – software for flow and transport modeling in variably saturated media. Groundwater, 48: 787–791.

Zeng C., Bennet G.D. (2002): Applied Contaminant Transport Modeling. New York, John Wiley & Sons Inc.: 621.

Wu S., Jeng D.-S., Seymour B.R. (2020): Numerical modelling of consolidation-induced solute transport in unsaturated soil with dynamic hydraulic conductivity and degree of saturation. Advances in Water Resources, 135: 103466.

Received: October 14, 2019
Accepted: September 3, 2020
Published online: December 30, 2020